

This is the accepted manuscript made available via CHORUS. The article has been published as:

Pressure-induced phase transition in
 $\text{La}_{1-x}\text{Sm}_x\text{O}_{0.5}\text{F}_{0.5}\text{BiS}_2$

Y. Fang, D. Yazici, B. D. White, and M. B. Maple

Phys. Rev. B **92**, 094507 — Published 15 September 2015

DOI: [10.1103/PhysRevB.92.094507](https://doi.org/10.1103/PhysRevB.92.094507)

Pressure-Induced Phase Transition in $\text{La}_{1-x}\text{Sm}_x\text{O}_{0.5}\text{F}_{0.5}\text{BiS}_2$

Y. Fang^{1,2}, D. Yazici^{2,3}, B. D. White^{2,3}, and M. B. Maple^{1,2,3*}

¹*Materials Science and Engineering Program, University of California, San Diego, La Jolla, California 92093, USA*

²*Center for Advanced Nanoscience, University of California, San Diego, La Jolla, California 92093, USA and*

³*Department of Physics, University of California, San Diego, La Jolla, California 92093, USA*

(Dated: August 20, 2015)

Electrical resistivity measurements on $\text{La}_{1-x}\text{Sm}_x\text{O}_{0.5}\text{F}_{0.5}\text{BiS}_2$ ($x = 0.1, 0.3, 0.6, 0.8$) have been performed under applied pressures up to 2.6 GPa from 2 K to room temperature. The superconducting transition temperature T_c of each sample significantly increases at a Sm-concentration dependent pressure P_t , indicating a pressure-induced phase transition from a low- T_c to a high- T_c phase. At ambient pressure, T_c increases dramatically from 2.8 K at $x = 0.1$ to 5.4 K at $x = 0.8$; however, the T_c values at $P > P_t$ decrease slightly with x and P_t shifts to higher pressures with Sm substitution. In the normal state, semiconducting-like behavior is suppressed and metallic conduction is induced with increasing pressure in all of the samples. These results suggest that the pressure dependence of T_c for the BiS_2 -based superconductors is related to the lattice parameters at ambient pressure and enable us to estimate the evolution of T_c for $\text{SmO}_{0.5}\text{F}_{0.5}\text{BiS}_2$ under pressure.

PACS numbers: 61.50.Ks, 74.25.F-, 74.62.Fj, 74.70.Dd

I. INTRODUCTION

The application of external pressure to materials has led to the discovery of many new superconductors and has apparently raised the record of the highest superconducting transition temperature, T_c , to 190 K in H_2S .¹ Due to its substantial impact on the crystalline and electronic structure of solids, applied pressure is recognized as a powerful tool to tune the T_c , critical fields, and other physical properties of superconductors.^{2,3} Recently, superconductivity with T_c values ranging from 2.7 to 10.6 K at ambient pressure has been reported for BiS_2 -based compounds including $\text{Bi}_4\text{O}_4\text{S}_3$, $\text{LnO}_{1-x}\text{F}_x\text{BiS}_2$ ($\text{Ln} = \text{La, Ce, Pr, Nd, Yb}$), $\text{La}_{1-x}\text{M}_x\text{OBiS}_2$ ($\text{M} = \text{Ti, Zr, Hf, Th}$), $\text{Sr}_{1-x}\text{La}_x\text{FBiS}_2$, EuBiS_2F , and $\text{Eu}_3\text{Bi}_2\text{S}_4\text{F}_4$.⁴⁻¹⁶ Similar to the cuprate and Fe-based superconductors, the structure of these compounds is characterized by alternate stacking of superconducting BiS_2 layers and charge-reservoir blocking layers, both of which are tunable by using chemical substitution or applying external pressure.^{4,5,11,14,17,18} Therefore, there is plenty of phase space to search for the optimal conditions for superconductivity in this family of compounds.

The compound $\text{LaO}_{0.5}\text{F}_{0.5}\text{BiS}_2$, synthesized under high pressure, was reported to have the highest T_c of ~ 10.6 K in contrast to the $T_c \sim 3$ K of the same compound when it is synthesized at ambient pressure.^{12,19} Although the crystal structure of both the sample annealed at ambient pressure (AP) and the one synthesized under applied high pressure (HP) have the same space group $P4/nmm$, the strongly reduced lattice parameters a and c are considered to be related to the enhancement in T_c of HP samples.^{12,19,20} On the other hand, $\text{LaO}_{0.5}\text{F}_{0.5}\text{BiS}_2$ (AP), which has a low T_c , undergoes a structural phase transition from tetragonal to monoclinic at a pressure of 0.7 GPa, and T_c is enhanced to 10.7 K.²¹ Similar abrupt increases in T_c were also observed in the compounds $\text{LnO}_{0.5}\text{F}_{0.5}\text{BiS}_2$ ($\text{Ln} = \text{Ce, Pr, Nd}$), $\text{LaO}_{0.5}\text{F}_{0.5}\text{BiSe}_2$, EuBiS_2F and $\text{Eu}_3\text{Bi}_2\text{S}_4\text{F}_4$ under pressure.²²⁻²⁶ A gradual increase in T_c up to 5.4 K was observed at ambient pressure in $\text{La}_{1-x}\text{Sm}_x\text{O}_{0.5}\text{F}_{0.5}\text{BiS}_2$ with increasing Sm concentration

until the solubility limit near $x = 0.8$.²⁷ The lattice parameter a in $\text{La}_{0.2}\text{Sm}_{0.8}\text{O}_{0.5}\text{F}_{0.5}\text{BiS}_2$ is significantly smaller compared with other BiS_2 based compounds; however, further optimization of superconductivity in this system is prevented by the presence of a solubility limit.²⁷ Hence, it would be interesting to explore the electrical transport properties of the system $\text{La}_{1-x}\text{Sm}_x\text{O}_{0.5}\text{F}_{0.5}\text{BiS}_2$ under pressure. Such an experiment will not only provide a broad picture of how T_c evolves at extreme conditions, but will also help to determine which parameters are essential to promote superconductivity in the BiS_2 -based compounds. Additionally, pressure may be particularly well suited to induce certain types of phase transitions in $\text{La}_{0.2}\text{Sm}_{0.8}\text{O}_{0.5}\text{F}_{0.5}\text{BiS}_2$ due to its extraordinarily small lattice parameters in ambient conditions.

II. EXPERIMENTAL DETAILS

The synthesis and crystal structure analysis of polycrystalline samples of $\text{La}_{1-x}\text{Sm}_x\text{O}_{0.5}\text{F}_{0.5}\text{BiS}_2$ are described elsewhere.^{10,27} The chemical composition of each sample presented in this paper is nominal; impurity phases, including $\text{La}(\text{Sm})\text{F}_3$, $\text{La}(\text{Sm})\text{O}$, and Bi_2S_3 , typically ~ 4 wt.% for $x = 0.1, 0.3, 0.6$ and ~ 8 wt.% for $x = 0.8$, were found in these samples, which may cause slight differences between the nominal and actual chemical compositions of the samples.²⁷ Geometric factors for each sample were measured before applying pressure and used to calculate the electrical resistivity from measurements of resistance. Electrical resistance measurements from ambient pressure to ~ 2.6 GPa were performed on samples with nominal Sm concentrations $x = 0.1, 0.3, 0.6, 0.8$ between 2 and 280 K using a standard four-probe method in a pumped ^4He dewar. External pressures were generated by a clamped piston-cylinder cell using a Teflon capsule filled with a 1:1 by volume mixture of n-pentane and isoamyl alcohol, which is known to be a good hydrostatic pressure medium.^{28,29} The pressures applied to the samples were inferred from the T_c of a high purity ($>99.99\%$) Sn disk inside the sample chamber of the cell using the well-

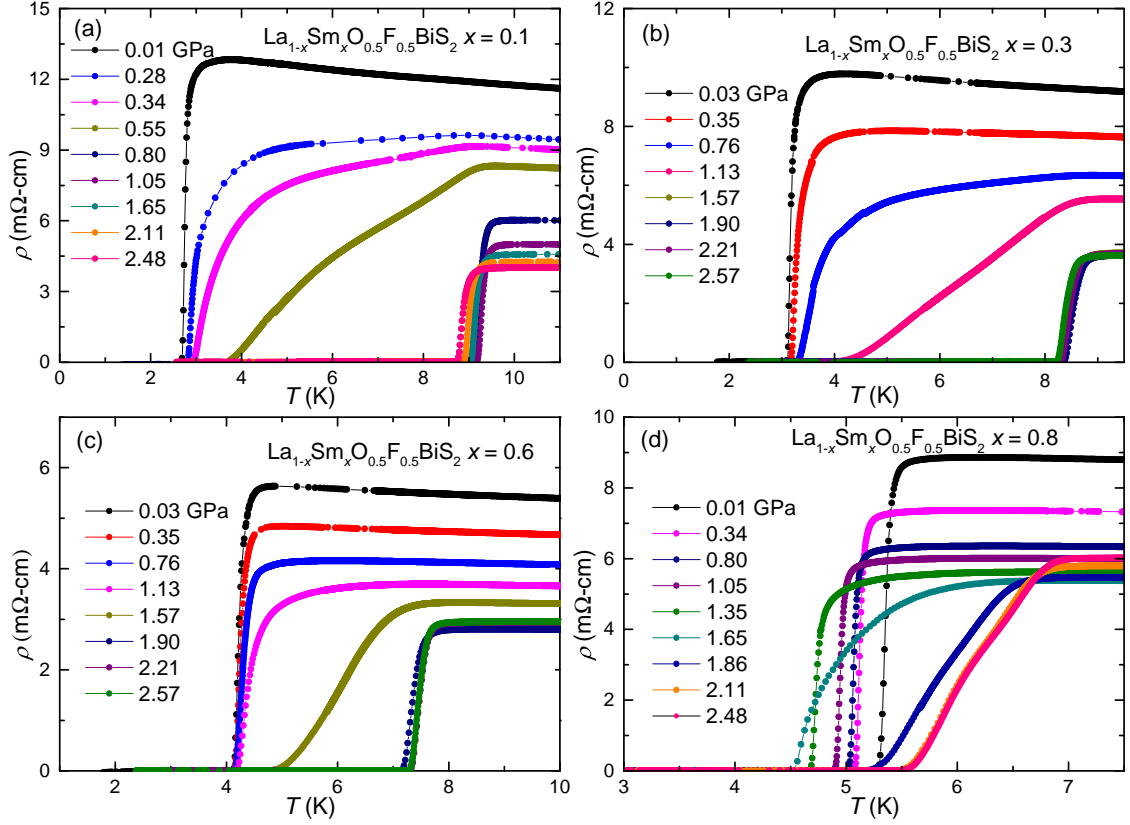


FIG. 1. (Color online) (a), (b), (c), (d) Temperature dependence of the electrical resistivity at various applied pressures near T_c for $\text{La}_{1-x}\text{Sm}_x\text{O}_{0.5}\text{F}_{0.5}\text{BiS}_2$ with $x = 0.1, 0.3, 0.6$, and 0.8 , respectively. Lines are guides to the eye.

established behavior of $T_c(P)$ in high purity Sn.³⁰ The width of the superconducting transition of Sn, indicated by an ac magnetic susceptibility measurement, is ~ 0.1 K at ambient pressure and remains the same until ~ 2.6 GPa. This result strongly suggests a good hydrostatic environment at low temperature and high pressure.

III. RESULTS AND DISCUSSION

Measurements of the low-temperature electrical resistivity $\rho(T)$ for $\text{La}_{1-x}\text{Sm}_x\text{O}_{0.5}\text{F}_{0.5}\text{BiS}_2$ ($x = 0.1, 0.3, 0.6, 0.8$) samples in zero magnetic field under applied pressures are depicted in Fig. 1. Superconducting (SC) transitions in which ρ abruptly drops from a finite value to zero were observed in each sample from ambient pressure to the highest pressure (~ 2.6 GPa) applied in this study. We defined T_c as the temperature where the electrical resistivity (ρ) falls to 50% of its normal-state value, and the width of the transition is characterized by identifying the temperatures where the electrical resistivity decreases to 90% and 10% of its normal state value. Superconducting transitions are very sharp at low pressures for all of the samples. However, as can be seen in Fig. 1, the width of the SC transition is quite broad within a narrow range of pressures (~ 0.5 GPa), after which, T_c is remarkably enhanced and the transitions become sharp again for the sam-

ples with nominal $x = 0.1, 0.3, 0.6$. In the case of the $x = 0.8$ sample, however, the width of the SC transition remains broad at high pressures after the enhancement in T_c ; this might be related to the $x = 0.8$ sample being so close to the solubility limit and possible chemical inhomogeneity of the sample.²⁷ This behavior reveals pressure-induced transitions from a low- T_c superconducting phase (SC1) to a high- T_c superconducting phase (SC2) in each sample.

The abrupt change in T_c under pressure is particularly apparent in the temperature-pressure phase diagram (see Fig. 2), in which P_t^o is the onset of the phase transition, P_t^c is the pressure where the phase transition is complete, and P_t is the midpoint between P_t^o and P_t^c . The broad superconducting transitions between P_t^o and P_t^c indicate the emergence of the SC2 phase; the sample in this pressure range is presumably in a mixture of the SC1 and SC2 phases. The values of T_c obtained in measurements with decreasing pressure (open symbols) are consistent with those measured with increasing pressure (filled symbols), revealing that the pressure-induced phase transitions are fully reversible. Tomita *et al.* recently reported a similar enhancement of T_c at ~ 0.7 GPa in polycrystalline samples of $\text{LaO}_{0.5}\text{F}_{0.5}\text{BiS}_2$, which was attributed to a structural phase transition from tetragonal to monoclinic due to sliding between two neighboring BiS_2 -layers along the a -axis.²¹ Since both $\text{LaO}_{0.5}\text{F}_{0.5}\text{BiS}_2$ and $\text{La}_{1-x}\text{Sm}_x\text{O}_{0.5}\text{F}_{0.5}\text{BiS}_2$ are characterized by the same

crystal structure with space group $P4/nmm$ at ambient pressure and have similar chemical compositions, it seems likely that the pressure-induced enhancement of T_c for $\text{La}_{1-x}\text{Sm}_x\text{O}_{0.5}\text{F}_{0.5}\text{BiS}_2$ is also associated with a structural phase transition, i.e., the SC1 phase is tetragonal in structure as has been demonstrated by Ref. 27 and SC2 phase is probably monoclinic.

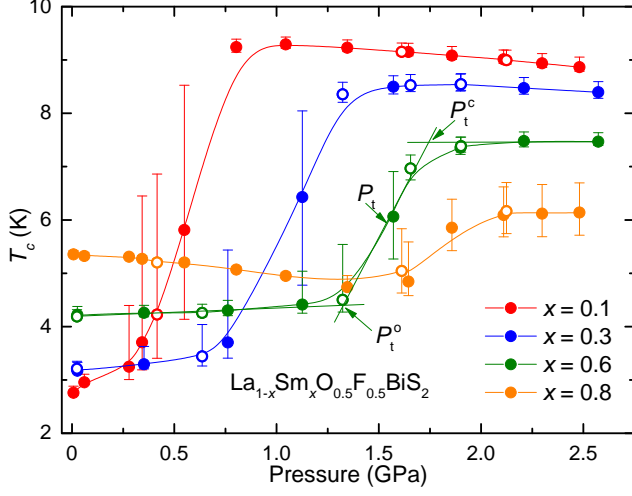


FIG. 2. (Color online) Superconducting critical temperature T_c vs pressure for $\text{La}_{1-x}\text{Sm}_x\text{O}_{0.5}\text{F}_{0.5}\text{BiS}_2$ ($x = 0.1, 0.3, 0.6, 0.8$). Filled and open circles with the same color represent T_c measured with increasing and decreasing pressure, respectively. The width of the superconducting transition is denoted by the vertical bars. P_t° and P_t^c are defined as the pressure of the low- T_c to high- T_c phase transition onsets and completions, respectively; P_t is the midpoint between P_t° and P_t^c .

The T_c values of $\text{La}_{1-x}\text{Sm}_x\text{O}_{0.5}\text{F}_{0.5}\text{BiS}_2$ superconductors at ambient pressure gradually increase from ~ 2.7 K for $x = 0.1$ to ~ 5.4 K for $x = 0.8$ with increasing Sm substitution up to the solubility limit near $x = 0.8$.²⁷ However, the pressure dependence of T_c for all of the samples at $P < P_t^\circ$ differ significantly from each other. For the $x = 0.1, 0.3, 0.6$ samples, T_c is initially enhanced with increasing pressure almost linearly and dT_c/dP decreases with increasing Sm concentration as is shown in Fig. 3 (right axis). Although the value of T_c for $x = 0.8$ is the highest among the four compositions at ambient pressure, dT_c/dP is negative with a value of roughly -0.45 K/GPa, which results in a decreasing T_c with pressure down to P_t° . These results suggest that reduction of the lattice parameter a , which is regarded to be essential to the enhancement of T_c for BiS₂-based compounds at ambient pressure,^{11,27,31,32} does not always result in an increase of T_c .

The T_c values at pressures just below and above the transition at P_t from SC1 to SC2 are plotted in Fig. 3 (left axis) and are denoted T_c° and T_c^c , respectively. Although T_c° increases with Sm substitution, T_c^c is suppressed almost linearly from 9.4 K for $x = 0.1$ to 6.2 K for $x = 0.8$, resulting in a reduction of the size of the jump in T_c below and above the phase transition (ΔT_c) with increasing Sm concentration. This phenomenon is very similar to that which was observed for the compounds $\text{LnO}_{0.5}\text{F}_{0.5}\text{BiS}_2$ ($\text{Ln} = \text{La, Ce, Pr, Nd}$),

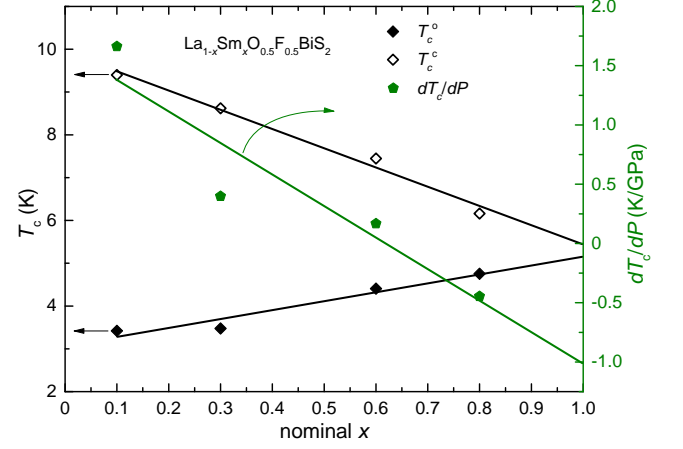


FIG. 3. (Color online) Sm concentration dependence of T_c at P_t° (T_c°) and at P_t^c (T_c^c) together with the initial rate of change in T_c with pressure (dT_c/dP) for $P < P_t^\circ$.

in which the T_c values above the phase transition decrease with increasing Ln atomic number.²² By linearly extrapolating both T_c° and T_c^c of $\text{La}_{1-x}\text{Sm}_x\text{O}_{0.5}\text{F}_{0.5}\text{BiS}_2$ to $x = 1$, the estimated ΔT_c of $\text{SmO}_{0.5}\text{F}_{0.5}\text{BiS}_2$ is only ~ 0.27 K, which is within the uncertainty of our estimate. If we plot ΔT_c for $\text{LnO}_{0.5}\text{F}_{0.5}\text{BiS}_2$, $\text{La}_{1-x}\text{Sm}_x\text{O}_{0.5}\text{F}_{0.5}\text{BiS}_2$, and the estimated ΔT_c for $\text{SmO}_{0.5}\text{F}_{0.5}\text{BiS}_2$ as a function of lattice parameter a , they are located almost on the same line despite the differences in their chemical composition (see Fig. 4(a)).

With Sm substitution for La, P_t increases from 0.59 GPa for $x = 0.1$ to 1.80 GPa for $x = 0.8$. The nearly linear evolution of P_t with Sm concentration (see Fig. 4(b)) enables one to estimate a P_t of ~ 2.2 GPa for $\text{SmO}_{0.5}\text{F}_{0.5}\text{BiS}_2$, which is consistent with the P_t values of other known $\text{LnO}_{0.5}\text{F}_{0.5}\text{BiS}_2$ compounds as is shown in the inset of Fig. 4(b).^{22,23} Figure 5 shows the T_c of $\text{La}_{1-x}\text{Sm}_x\text{O}_{0.5}\text{F}_{0.5}\text{BiS}_2$ at different pressures and Sm concentrations together with the estimated T_c of $\text{SmO}_{0.5}\text{F}_{0.5}\text{BiS}_2$ under pressure. The T_c at pressures below and above 2.2 GPa of $\text{SmO}_{0.5}\text{F}_{0.5}\text{BiS}_2$ is estimated from a linear extrapolation of the T_c values of the four samples below and above the phase transition, respectively. It can be seen that higher T_c values for the SC1 phase are found at higher Sm concentrations and lower pressures; however, higher T_c values for the SC2 phase are located in the region with lower Sm concentration just above the phase transition. In fact, by further reducing the Sm concentration to $x = 0$, a higher T_c value of ~ 10.7 K could be obtained under pressure in $\text{LaO}_{0.5}\text{F}_{0.5}\text{BiS}_2$, which has the largest a lattice parameter among the $\text{LnO}_{0.5}\text{F}_{0.5}\text{BiS}_2$ compounds at ambient pressure.²¹ On the other hand, reducing a enhances T_c at ambient pressure; however, it also reduces ΔT_c as discussed above. The pressure dependence of T_c below and above 2.2 GPa for $\text{SmO}_{0.5}\text{F}_{0.5}\text{BiS}_2$ has a similar trend and is almost indistinguishable as is shown in Fig. 5. Thus, the possibility that $\text{SmO}_{0.5}\text{F}_{0.5}\text{BiS}_2$ has the same phase at low and high pressures cannot be ruled out. Although it was reported that $\text{SmO}_{0.5}\text{F}_{0.5}\text{BiS}_2$ can be synthesized by solid state reaction,³³ this result might be helpful in explaining why this parent com-

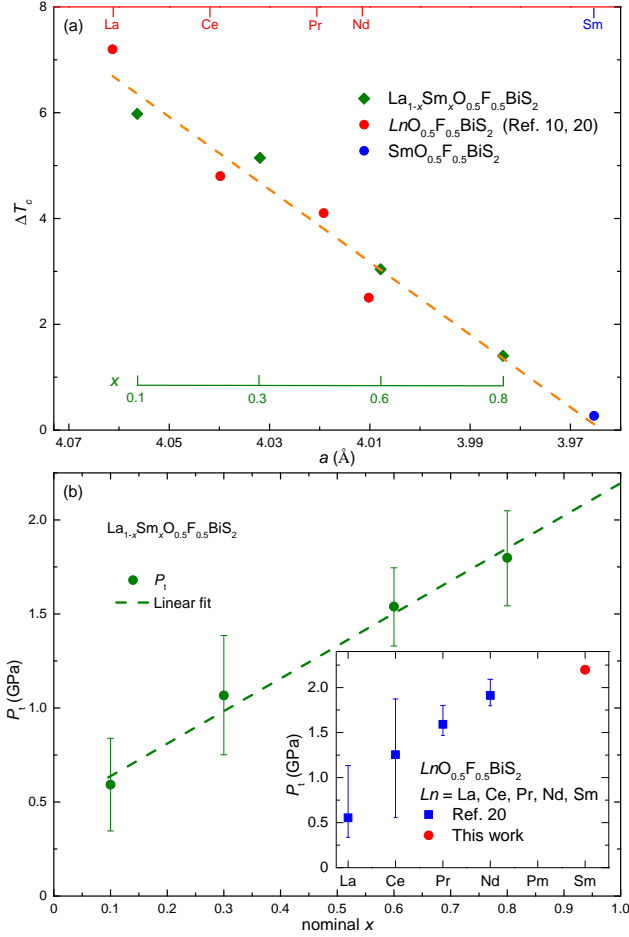


FIG. 4. (Color online) Dependence of (a) ΔT_c on lattice parameter a and (b) dependence of P_t on nominal Sm concentration. The inset in panel (b) displays the evolution of P_t as a function of Ln . Dashed lines are guides to the eye.

pound could not be synthesized in other studies using the same method.^{27,31}

As is shown in Fig. 6, $\rho(T)$ of $\text{La}_{1-x}\text{Sm}_x\text{O}_{0.5}\text{F}_{0.5}\text{BiS}_2$ increases with decreasing temperature at low pressures in their normal state, indicating semiconducting-like behavior, which is suppressed by applied pressure. However, as the representative $\rho(T)$ data in the inset of Fig. 6(d) show, a minimum near 262 K (T_{\min}) emerges at pressures above 0.4 GPa. Semiconducting-like behavior is observed in $\rho(T)$ for $T < T_{\min}$. T_{\min} decreases with increasing pressure and then saturates at ~ 1.8 GPa, reaching a value of roughly 40 K. Except for the $x = 0.1$ sample, in which T_{\min} does not saturate until ~ 2.5 GPa, similar behavior is observed in the other samples under high pressures. However, the relationship between T_{\min} and Sm concentration is still unclear. The appearance of a metallic-like to semiconducting-like cross over was also found in $\text{Eu}_3\text{Bi}_2\text{S}_4\text{F}_4$, $\text{Sr}_{1-x}\text{La}_x\text{FBiS}_2$ ($x \geq 0.45$), LaOBiS_2 , and ThOBiS_2 at ambient pressure. In the first example, this behavior was attributed to a self-doping effect arising from Eu intermediate valence, while in the second exam-

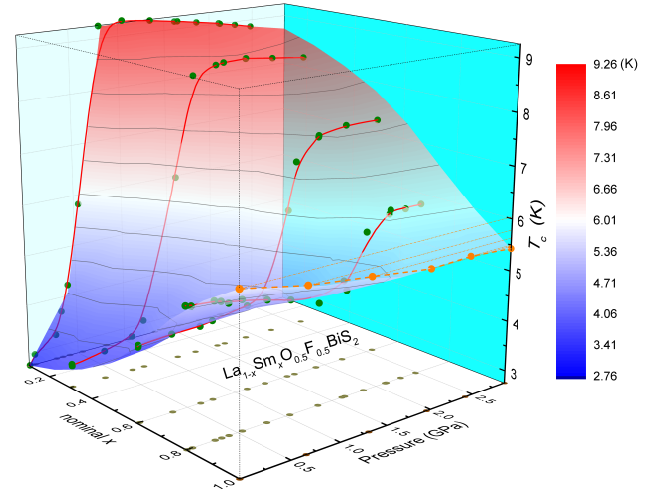


FIG. 5. (Color online) T_c plotted as a function of pressure and nominal Sm concentration x . The T_c of $\text{SmO}_{0.5}\text{F}_{0.5}\text{BiS}_2$ is estimated by linearly extrapolating the T_c of $\text{La}_{1-x}\text{Sm}_x\text{O}_{0.5}\text{F}_{0.5}\text{BiS}_2$ ($x = 0.1, 0.3, 0.6, 0.8$) below and above the phase transition near P_t . Filled circles in the x - y plane are projections of T_c .

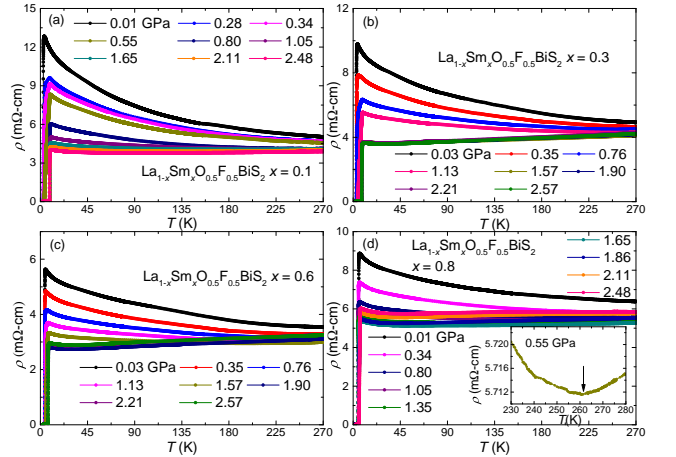


FIG. 6. (Color online) (a), (b), (c), (d) Electrical resistivity of $\text{La}_{1-x}\text{Sm}_x\text{O}_{0.5}\text{F}_{0.5}\text{BiS}_2$ with $x = 0.1, 0.3, 0.6$, and 0.8 under applied pressure from 270 K to ~ 1.2 K, respectively. The inset of panel (d) is a representative $\rho(T)$ curve in which a minimum (indicated by the arrow) is observed in the normal state upon cooling.

ple, it was ascribed to Anderson localization.^{13,16,34} However, further work is required to identify the origin of the minimum in $\text{La}_{1-x}\text{Sm}_x\text{O}_{0.5}\text{F}_{0.5}\text{BiS}_2$ since the valence of Sm ions might change and sample defects might develop at high pressures.

Figure 7 shows ρ values at 270 K ($\rho_{270\text{K}}$) and at certain low temperatures (ρ_{low}), explicitly indicated in the figure, just higher than T_c for each sample. Both $\rho_{270\text{K}}$ and ρ_{low} first decrease with increasing pressure almost linearly. However, the slope of the $\rho(P)$ curve changes at the pressure indicated by the arrows in Fig. 7, resulting in a kink for each $\rho(P)$ curve. For the $x = 0.6$ and 0.8 samples, a positive pressure coefficient of resistivity is observed at the pressures above the kink. Although the kink is located at pressures near P_t , it should

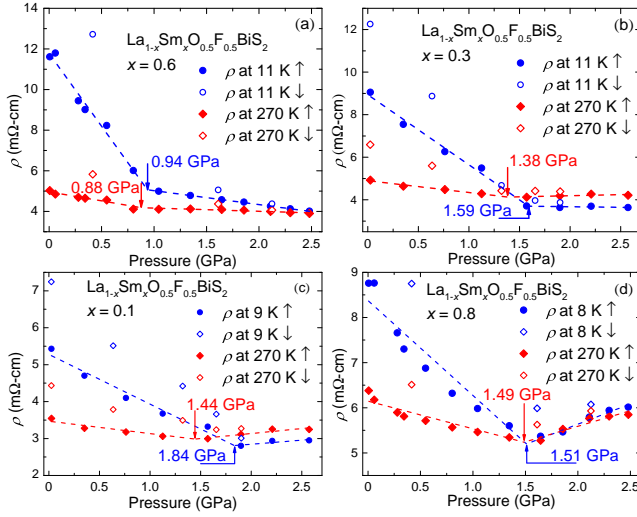


FIG. 7. (Color online) (a), (b), (c), (d) Electrical resistivity of $\text{La}_{1-x}\text{Sm}_x\text{O}_{0.5}\text{F}_{0.5}\text{BiS}_2$ with $x = 0.1, 0.3, 0.6$, and 0.8 , respectively, at a temperature just above T_c in the normal state and at 270 K. The filled circles represent data collected with increasing pressure and the open circles are the data taken upon releasing the pressure. The dashed lines, which are guides to the eye, reflect the slopes of the pressure dependence of the electrical resistivity. Arrows indicate the pressure at which the slope changes.

be noted that the kink does not necessarily coincide with the appearance of the SC2 phase, since both the phase transition between SC1 to SC2 and the appearance of metallic-like behavior may contribute to the normal-state electrical resistivity of the samples.

Since the electrical transport behavior of single crystals of $\text{La}_{1-x}\text{Sm}_x\text{O}_{0.5}\text{F}_{0.5}\text{BiS}_2$ has not yet been reported, it is still difficult to determine whether the observed semiconducting-like behavior is related to poor intergrain contact or whether it is an intrinsic property. If we assume that the semiconducting-like behavior is intrinsic, the energy gap can be estimated by using the simple activation-type relation:

$$\rho(T) = \rho_0 e^{\Delta/2k_B T}, \quad (1)$$

where ρ_0 is a constant, k_B is the Boltzmann constant, and Δ is the energy gap.^{35,36} Because the relationship between $1/T$ and $\ln \rho$ is not linear for the whole temperature range in the normal state, the $\rho(T)$ data were fitted using Eq. (1) in two different temperature ranges, 270-160 K and 22-10 K, similar to the analysis in Refs. 22, 23, 35, and 36. The energy gaps Δ_1/k_B and Δ_2/k_B , which are extracted from the high temperature and low temperature ranges, respectively, are plotted in Fig. 8. The gap Δ_1/k_B is not shown above the pressure at which metallic-like conduction is observed. It can be seen that both Δ_1/k_B and Δ_2/k_B are suppressed rapidly with increasing pressure; however, the value of Δ_1/k_B does not change significantly above P_t^c with increasing pressure for all of the samples. Hence, the SC2 phase probably has a different band structure which is less sensitive to pressure.

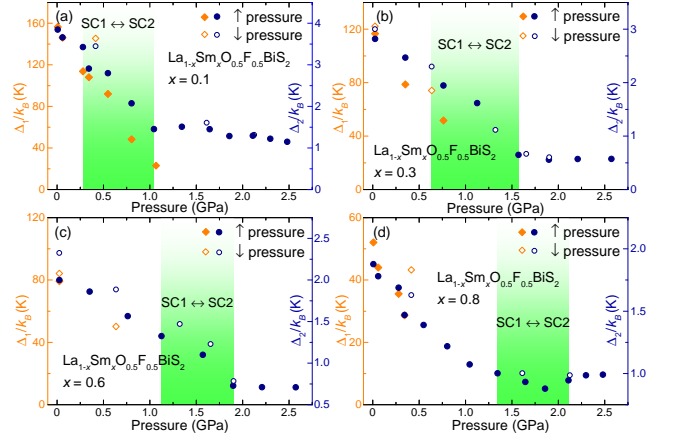


FIG. 8. (Color online) (a), (b), (c), (d) Evolution of the energy gaps Δ_1/k_B and Δ_2/k_B plotted as a function of pressure for $x = 0.1, 0.3, 0.6$, and 0.8 , respectively. Filled and open symbols represent values that were obtained with increasing and decreasing pressure, respectively. Pressure ranges in which the low- T_c to high- T_c phase transition is observed and in which the normal-state electrical resistivity shows metallic-like behavior above 40 K are also indicated.

Although T_c is reversible (i.e., there is no difference in values measured for increasing and decreasing pressure), values of Δ_1/k_B and Δ_2/k_B are higher for decreasing pressure than increasing pressure, indicating an enhancement of semiconducting-like behavior for all of the samples. A similar phenomenon was also observed in $\text{LaO}_{0.5}\text{F}_{0.5}\text{BiS}_2$ and $\text{CeO}_{0.5}\text{F}_{0.5}\text{BiS}_2$.²³ This behavior is associated with the pressure dependence of the electrical resistivity in which values of ρ obtained at similar pressures in measurements in which the pressure cell was being unloaded are significantly higher than those measured upon loading as the representative data show in Fig. 7. However, irreversible defects and disorder as well as a reduction of the geometric factors might develop in the samples under high pressures, which could contribute to a reduction in the conductivity of the samples. Since the energy gap Δ_1/k_B and Δ_2/k_B are derived from the electronic structure, there is no obvious reason why these fundamental quantities should show hysteretic behavior as a function of pressure.

IV. SUMMARY

Electrical resistivity measurements on polycrystalline samples of the BiS_2 -based superconductors $\text{La}_{1-x}\text{Sm}_x\text{O}_{0.5}\text{F}_{0.5}\text{BiS}_2$ ($x = 0.1, 0.3, 0.6, 0.8$) were performed from 2 K to room temperature under applied pressures. In the normal state, semiconducting-like behavior is suppressed with increasing pressure. A reversible low- T_c to high- T_c superconductor phase transition was observed in all of the samples at a pressure that is proportional to the Sm concentration. With increasing Sm concentration, ΔT_c is suppressed and a larger pressure is necessary to induce the transition from the SC1 to the SC2 phase. It is also found that an optimal T_c could be tuned by decreasing the a

lattice parameter in the SC1 phase at ambient pressure or by increasing a in the SC2 phase under pressure. These results indicate that the high-pressure behavior of Sm-substituted $\text{LaO}_{0.5}\text{F}_{0.5}\text{BiS}_2$ is largely determined by Sm concentration or the lattice parameter a at ambient pressure. Therefore, the evolution of T_c under pressure for the parent compound $\text{SmO}_{0.5}\text{F}_{0.5}\text{BiS}_2$ can be estimated, and we find that the SC1 and SC2 phases exhibit almost indistinguishable T_c values; this result suggests that applied pressure may not induce a phase transition in $\text{SmO}_{0.5}\text{F}_{0.5}\text{BiS}_2$.

ACKNOWLEDGMENTS

Electrical resistivity measurements under applied pressure were supported by the National Nuclear Security Administration under the Stewardship Science Academic Alliance Program through the US Department of Energy (DOE) under Grant No. DE-NA0001841. Sample synthesis and characterization at ambient pressure were supported by the U. S. Department of Energy, Office of Basic Energy Sciences, Division of Materials Sciences and Engineering under Grant No. DE-FG02-04-ER46105. Helpful discussions with I. Jeon and C. T. Wolowiec are gratefully acknowledged.

-
- * Corresponding Author: mbmaple@ucsd.edu
- ¹ A. P. Drozdov, M. I. Erements, and I. A. Troyan, arXiv preprint arXiv:1412.0460 (2014).
 - ² K. Shimizu, K. Amaya, and N. Suzuki, J. Phys. Soc. Jpn **74**, 1345 (2005).
 - ³ A. S. Sefat, Rep. Prog. Phys. **74**, 124502 (2011).
 - ⁴ Y. Mizuguchi, H. Fujihisa, Y. Gotoh, K. Suzuki, H. Usui, K. Kuroki, S. Demura, Y. Takano, H. Izawa, and O. Miura, Phys. Rev. B **86**, 220510 (2012).
 - ⁵ S. K. Singh, A. Kumar, B. Gahtori, G. Sharma, S. Patnaik, and V. P. S. Awana, J. Am. Chem. Soc. **134**, 16504 (2012).
 - ⁶ V. P. S. Awana, A. Kumar, R. Jha, S. Kumar Singh, A. Pal, J. Saha, and S. Patnaik, Solid State Commun. **157**, 21 (2013).
 - ⁷ S. Demura, Y. Mizuguchi, K. Deguchi, H. Okazaki, H. Hara, T. Watanabe, S. James Denholme, M. Fujioka, T. Ozaki, H. Fujihisa, G. Yoshito, M. Osuke, Y. Takahide, T. Hiroyuki, and T. Yoshihiko, J. Phys. Soc. Jpn. **82**, 033708 (2013).
 - ⁸ Y. Mizuguchi, S. Demura, K. Deguchi, Y. Takano, H. Fujihisa, Y. Gotoh, H. Izawa, and O. Miura, J. Phys. Soc. Jpn. **81**, 114725 (2012).
 - ⁹ J. Xing, S. Li, X. Ding, H. Yang, and H.-H. Wen, Phys. Rev. B **86**, 214518 (2012).
 - ¹⁰ D. Yazici, K. Huang, B. D. White, A. H. Chang, A. J. Friedman, and M. B. Maple, Phil. Mag. **93**, 673 (2013).
 - ¹¹ Y. Mizuguchi, Physics Procedia **58**, 94 (2014).
 - ¹² K. Deguchi, Y. Mizuguchi, S. Demura, H. Hara, T. Watanabe, S. Denholme, M. Fujioka, H. Okazaki, T. Ozaki, H. Takeya, T. Yamaguchi, O. Miura, and Y. Takano, Europhys. Lett. **101**, 17004 (2013).
 - ¹³ D. Yazici, K. Huang, B. D. White, I. Jeon, V. W. Burnett, A. J. Friedman, I. K. Lum, M. Nallaiyan, S. Spagna, and M. B. Maple, Phys. Rev. B **87**, 174512 (2013).
 - ¹⁴ X. Lin, X. X. Ni, B. Chen, X. F. Xu, X. X. Yang, J. H. Dai, Y. K. Li, X. J. Yang, Y. K. Luo, Q. Tao, G. H. Cao, and Z. Xu, Phys. Rev. B **87**, 020504 (2013).
 - ¹⁵ H. F. Zhai, Z. T. Tang, H. Jiang, K. Xu, K. Zhang, P. Zhang, J. K. Bao, Y. L. Sun, W. H. Jiao, I. Nowik, I. Felner, Y. K. Li, X. F. Xu, Q. Tao, C. M. Feng, Z. A. Xu, and G. H. Cao, Phys. Rev. B **90**, 064518 (2014).
 - ¹⁶ H. F. Zhai, P. Zhang, S. Q. Wu, C. Y. He, Z. T. Tang, H. Jiang, Y. L. Sun, J. K. Bao, I. Nowik, I. Felner, Y. W. Zeng, Y. K. Li, X. F. Xu, Q. Tao, Z. A. Xu, and G. H. Cao, J. Am. Chem. Soc. **136**, 15386 (2014).
 - ¹⁷ D. Yazici, I. Jeon, B. D. White, and M. B. Maple, Physica C **514**, 218 (2015).
 - ¹⁸ Y. Mizuguchi, J. Phys. Chem. Solids **84**, 34 (2015).
 - ¹⁹ Y. Mizuguchi, T. Hiroi, J. Kajitani, H. Takatsu, H. Kadowaki, and O. Miura, J. Phys. Soc. Jpn. **83**, 053704 (2014).
 - ²⁰ I. Pallecchi, G. Lamura, M. Putti, J. Kajitani, Y. Mizuguchi, O. Miura, S. Demura, K. Deguchi, and Y. Takano, Phys. Rev. B **89**, 214513 (2014).
 - ²¹ T. Tomita, M. Ebata, H. Soeda, H. Takahashi, H. Fujihisa, Y. Gotoh, Y. Mizuguchi, H. Izawa, O. Miura, S. Demura, K. Deguchi, and Y. Takano, J. Phys. Soc. Jpn. **83**, 063704 (2014).
 - ²² C. T. Wolowiec, B. D. White, I. Jeon, D. Yazici, K. Huang, and M. B. Maple, J. Phys.: Condens. Matter **25**, 422201 (2013).
 - ²³ C. T. Wolowiec, D. Yazici, B. D. White, K. Huang, and M. B. Maple, Phys. Rev. B **88**, 064503 (2013).
 - ²⁴ Y. K. Luo, H. F. Zhai, P. Zhang, Z. A. Xu, G. H. Cao, and J. D. Thompson, Phys. Rev. B **90**, 220510 (2014).
 - ²⁵ J. Z. Liu, S. Li, Y. F. Li, X. Y. Zhu, and H.-H. Wen, Phys. Rev. B **90**, 094507 (2014).
 - ²⁶ C. Y. Guo, Y. Chen, M. Smidman, S. A. Chen, W. B. Jiang, H. F. Zhai, Y. F. Wang, G. H. Cao, J. M. Chen, X. Lu, and H. Q. Yuan, Phys. Rev. B **91**, 214512 (2015).
 - ²⁷ Y. Fang, D. Yazici, B. D. White, and M. B. Maple, Phys. Rev. B **91**, 064510 (2015).
 - ²⁸ T. F. Smith, C. W. Chu, and M. B. Maple, Cryogenics **9**, 53 (1969).
 - ²⁹ A. Jayaraman, A. R. Hutson, J. H. McFee, A. S. Coriell, and R. G. Maines, Rev. Sci. Instrum. **38**, 44 (1967).
 - ³⁰ T. Smith, C. W. Chu, and M. B. Maple, Cryogenics **9**, 53 (1969).
 - ³¹ J. Kajitani, T. Hiroi, A. Omachi, O. Miura, and Y. Mizuguchi, J. Phys. Soc. Jpn. **84**, 044712 (2015).
 - ³² J. Kajitani, A. Omachi, T. Hiroi, O. Miura, and Y. Mizuguchi, Physica C **504**, 33 (2014).
 - ³³ G. S. Thakur, G. K. Selvan, Z. Haque, L. C. Gupta, S. L. Samal, S. Arumugam, and A. K. Ganguli, Inorg. Chem. **54**, 1076 (2015).
 - ³⁴ H. Sakai, D. Kotajima, K. Saito, H. Wadati, Y. Wakisaka, M. Mizumaki, K. Nitta, Y. Tokura, and S. Ishiwata, J. Phys. Soc. Jpn. **83**, 014709 (2014).
 - ³⁵ H. Kotegawa, Y. Tomita, H. Tou, H. Izawa, Y. Mizuguchi, O. Miura, S. Demura, K. Deguchi, and Y. Takano, J. Phys. Soc. Jpn. **81**, 103702 (2012).
 - ³⁶ I. Jeon, D. Yazici, B. D. White, A. J. Friedman, and M. B. Maple, Phys. Rev. B **90**, 054510 (2014).